Nonmonotonic effects of nonreciprocal interactions on glass transition and diffusion in a two-dimensional emergent active system

Rui-xue Guo,[1,2] Jia-jian Li,[1,2] Chun-hua Zeng,[3,*] Ya-feng He,[4,†] and Bao-quan Ai[1,2,‡]

[1]*Key Laboratory of Atomic and Subatomic Structure and Quantum Control (Ministry of Education), Guangdong Basic Research Center of Excellence for Structure and Fundamental Interactions of Matter, School of Physics, South China Normal University, Guangzhou 510006, China*

[2]*Guangdong Provincial Key Laboratory of Quantum Engineering and Quantum Materials, and Guangdong-Hong Kong Joint Laboratory of Quantum Matter, South China Normal University, Guangzhou 510006, China*

[3]*Faculty of Science, Kunming University of Science and Technology, Kunming 650500, China*

[4]*College of Physics Science and Technology, Hebei University, Baoding 071002, China*

(Received 19 May 2025; accepted 15 September 2025; published 1 October 2025)

The glass transition of supercooled liquids poses a significant challenge in statistical physics. Although the glass transition has been extensively investigated in various active systems, the influence of nonreciprocal interactions between particles on this transition remains an open question. In this study, we investigate the diffusion and glass transition within a two-dimensional Kob-Andersen mixture featuring nonreciprocal particle interactions. Our findings reveal that nonreciprocity among particles profoundly impacts the system's dynamics. Specifically, in the gaseous or high-temperature liquid phase, the diffusion coefficient exhibits a consistent increase with rising nonreciprocity. However, in the viscous liquid or glassy state, the emergence of large-scale directed motion leads to a weakly nonmonotonic relationship between the diffusion coefficient and nonreciprocity. As nonreciprocity increases, the diffusion coefficient experiences a decline, reaching a minimum at finite nonreciprocity. Under dense conditions and at low temperatures, the system undergoes a transition between the glassy and liquid states by modulating nonreciprocity. However, at high temperatures, nonreciprocity becomes less significant, and this transition cannot be achieved by changing nonreciprocity. Our findings shed light on the intricate interplay between particle interactions and system dynamics in the context of glass transition phenomena.

DOI: 10.1103/vncw-4jjt

I. INTRODUCTION

The glass transition is a phenomenon in which a liquidlike state transitions to a solidlike state without crystallization [1,2]. The glassy state is characterized by several distinctive features: prolonged relaxation times in the intermediate scattering function, subdiffusive behavior in the mean square displacement (MSD) during the intermediate regime, and non-Gaussian distributions in particle displacement, among others [3–9]. Recently, it has been observed that by increasing the density to high values, self-propelled systems can enter dynamically arrested or active glassy states, exhibiting remarkable similarities to conventional passive ones [10]. These phenomena have been notably observed in synthetic colloidal assemblies [11], living cells and cell layers [12–14], and various simulations and theoretical studies [15–33]. The exploration of active glassy states and their interrelation with conventional passive counterparts has gained momentum, positioned at the intersection of active matter and glassy physics.

Increasing evidence from both biological and synthetic systems shows that particle interactions are not necessarily reciprocal at the coarse-grained level. Nonreciprocal behaviors have been observed across a broad range of scales, from microscale interactions among bacteria [34] to macroscale collective motion in animal herds [35]. In engineered systems, such as suspensions of magnetic microdisks, the action-reaction symmetry can be intentionally broken through hydrodynamic coupling [36]. These phenomena are commonly observed in nonequilibrium systems, primarily originating from external driving of the medium and variations in how different particle species interact with the surrounding environment. Consequently, in nonequilibrium environments, particles may exhibit effective asymmetric interactions that appear to violate the principle of action-reaction symmetry [34–47]. Notably, nonreciprocal interaction schemes can induce collective chiral motion, which is sustained as long as the angular velocity of the rotating particles remains below a specified threshold [47].

Moreover, nonreciprocal interactions may provoke persistent active motion, similar to the dynamics observed

*Contact author: zchh2009@126.com
†Contact author: heyf@hbu.edu.cn
‡Contact author: aibq@scnu.edu.cn

in conventional active particle models [46]. Recent studies [17–21] have explored the active fluidization behavior in glassy systems. For instance, Mandal *et al.* [21] analyzed the active fluidization phenomena in dense glassy systems at low temperatures, demonstrating how the introduction of activity or self-propulsion force leads to the breaking and fluidization of cage structures, ultimately resulting in the disappearance of the glassy phase upon exceeding a critical value. Although pairs of particles with nonreciprocal interactions can temporarily behave like self-driven dimers, nonreciprocity is fundamentally different from self-propulsion mechanisms. Specifically, (1) in nonreciprocal systems, interactions are asymmetric, meaning the interaction strength between two individuals is different, which may lead to traveling states [38,43]. (2) Nonreciprocal systems lack features commonly used in active systems, such as persistence time and fixed self-propulsion speed. Consequently, nonreciprocal interactions may significantly influence particle diffusion and motion. This leads to a pivotal question: How do nonreciprocal interactions affect particle diffusion and drive the system toward a transition into arrested or active glassy states?

To tackle this question, we have investigated the diffusion and glass dynamics of a binary mixture of Brownian particles with nonreciprocal interactions. We discovered that these interactions have a profound impact on particle dynamics. In terms of diffusion behavior, when the system is in a gaseous or high-temperature liquid state, the diffusion coefficient increases monotonically with rising nonreciprocity. Conversely, in the viscous liquid or glassy state, due to the emergence of directional motion, the relationship between the diffusion coefficient and nonreciprocity becomes nonmonotonic. With increasing nonreciprocity, the diffusion coefficient exhibits a local minimum before rising again. Regarding the glass transition under dense conditions, at low temperatures, the system can transition between the glassy and liquid states by modulating nonreciprocity. However, at high temperatures, the influence of nonreciprocity diminishes, rendering the transition inaccessible via adjustments in nonreciprocity alone.

II. MODEL AND METHODS

We consider a two-dimensional Kob-Andersen mixture consisting of two types of particles, A and B, in a number ratio of 65:35 to avoid crystallization [7]. It is worth noting that this ratio differs from the standard 80:20 composition commonly used in the three-dimensional Kob-Andersen model. These particles are confined in a two-dimensional box of size $L \times L$, moving within periodic boundary conditions. Hydrodynamic interactions and inertia are not taken into consideration. The dynamics of particle i is described by the following overdamped Langevin equation:

$$\frac{d\mathbf{r}_i}{dt} = \mu \sum_{j \neq i} \mathbf{F}_{ij} + \sqrt{2\mu k_B T}\xi_i(t), \tag{1}$$

where $\mathbf{r}_i = (x_i, y_i)$ represents the central position of particle i. T is the temperature, k_B is the Boltzmann constant, and μ is the mobility. $\xi_i(t)$ represents Gaussian white noise with unit variance and zero mean.

The interaction potential between particles is represented by the truncated and shifted Lennard-Jones potential. For two particles α and β (where $\alpha, \beta \in \{A, B\}$), their interaction potential is described as follows:

$$U_{\alpha\beta} = \begin{cases} 4\epsilon_{\alpha\beta}\left[\left(\frac{\sigma_{\alpha\beta}}{r}\right)^{12} - \left(\frac{\sigma_{\alpha\beta}}{r}\right)^{6} + C_{\text{shift}}\right], & r \leqslant 2.5\sigma_{\alpha\beta}, \\ 0, & r > 2.5\sigma_{\alpha\beta}, \end{cases} \tag{2}$$

where the constants ϵ and σ determine the energy unit and length unit, respectively. Its characteristics are characterized by parameters $\sigma_{AA} = 1, \sigma_{AB} = 0.8, \sigma_{BB} = 0.88, \epsilon_{AA} = 1, \epsilon_{AB} = 1.5$, and $\epsilon_{BB} = 0.5$. In this case, we set $C_{\text{shift}} = (\frac{2}{5})^6 - (\frac{2}{5})^{12}$ to ensure that the potential remains continuous at cutoff radius $r = 2.5\sigma_{\alpha\beta}$. Here, we select parameters of the standard Kob-Andersen mixture, which facilitates the simulation of glassy states and glass transitions. The inclusion of particles with different sizes aims to prevent crystallization of the system at low temperatures and high densities. As a classical model for glass formation, the Kob-Andersen model has been widely applied to investigate the dynamical behavior of binary mixtures and is highly recognized and referenced in academia.

We consider the interaction between particles to be nonreciprocal, which violates Newton's third law. This phenomenon can be observed in many life and natural systems [34,35,40–45]. We adopted the nonreciprocal interaction model proposed by Chiu and Omar in their study [43]. They explored the impact of nonreciprocal interactions on system phase behavior and proposed a model system for which the degree of nonreciprocity can be continuously adjusted. The findings revealed that nonreciprocal interactions impact phase behavior in unexpected ways, which is crucial for the advancement of multicomponent nonequilibrium coexistence theories.

Extending this model, the force $\mathbf{F}_{ij}(r)$ exerted by particle j on particle i takes the form [43]

$$\mathbf{F}_{ij}(\mathbf{r}) = \mathbf{F}^C_{ij}(\mathbf{r}) \times \begin{cases} 1 - \Delta(r), & i = A, \quad j = B, \\ 1 + \Delta(r), & i = B, \quad j = A, \\ 1, & i = j = A \quad \text{or } i = j = B, \end{cases} \tag{3}$$

where $\mathbf{F}^C_{ij}(\mathbf{r}) = -\nabla_i U_{\alpha\beta}$ is a conservative force that obeys Newton's third law, implying $\mathbf{F}^C_{ij}(\mathbf{r}) = -\mathbf{F}^C_{ji}(\mathbf{r})$. Here, i and j are particle indices. The first line applies when i is type A and j is type B, and the other two lines follow similarly. Specifically,

(1) For particles belonging to the same species, the interaction remains reciprocal: $\mathbf{F}_{ij}(\mathbf{r}) = \mathbf{F}^C_{ij}(\mathbf{r})$.

(2) For particles of different species, the interaction includes both a reciprocal component, $\mathbf{F}^R_{ij}(\mathbf{r}) = \mathbf{F}^C_{ij}(\mathbf{r})$, and a nonreciprocal component, $\mathbf{F}^{\text{NR}}_{ij}(\mathbf{r}) = \pm\Delta(r) \times \mathbf{F}^C_{ij}(\mathbf{r})$.

As a result, interactions between different particle types produce a net force

$$\mathbf{F}^{\text{NR}}_{\text{net}}(\mathbf{r}) = \mathbf{F}_{ij}(\mathbf{r}) + \mathbf{F}_{ji}(\mathbf{r}) = 2\mathbf{F}^{\text{NR}}_{ij}(\mathbf{r}) = 2\Delta(r)\mathbf{F}^C_{ij}(\mathbf{r}), \tag{4}$$

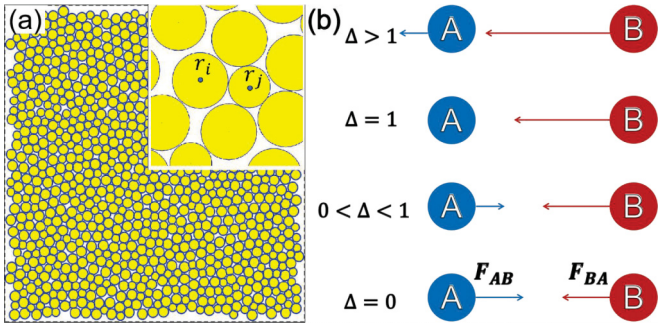

FIG. 1. (a) Schematic diagram containing particles of types A and B (drawing inspiration from Ref. [43]). (b) Schematic diagram of pairwise nonreciprocal interactions [as shown in Eq. (3)] between different species A and B. The system is reciprocal for $\Delta = 0$ and becomes a predator-prey state for $\Delta > 1$.

which can be interpreted as an emergent active force induced by internal nonreciprocity. Its strength depends on the particle arrangement and the form of $\Delta(r)$.

To simplify the model, we employ a step-function representation for the nonreciprocity form [43]:

$$\Delta(r) = \begin{cases} 0, & r < d_{\text{rec}}, \\ \Delta, & r \geqslant d_{\text{rec}}. \end{cases} \tag{5}$$

Here d_{rec} defines the threshold beyond which particle interactions become nonreciprocal: (1) For $r < d_{\text{rec}}$, the interaction remains entirely reciprocal with no nonreciprocal contribution and (2) for $r \geqslant d_{\text{rec}}$, a constant degree of nonreciprocity Δ is introduced. In this work, we set $d_{\text{rec}} = 2^{1/6}\sigma_{\alpha\beta}$, which corresponds to the demarcation point between repulsive and attractive forces. We control nonreciprocity solely through the attractive part of the interactions, which is done without loss of generality. Introducing nonreciprocity in both the attractive and repulsive parts does not qualitatively affect the results. Furthermore, this approach offers significant simplifications in numerical simulations. Since repulsive forces between particles are significant only at very short distances and must prevent particles from overlapping, neglecting nonreciprocity in the repulsive part simplifies the computational process and enhances efficiency. Moreover, considering nonreciprocity in the repulsive force can easily lead to unstable numerical calculations.

The paired nonreciprocal interactions between particles of different types, as illustrated in Fig. 1(b), exhibit distinct regimes depending on the parameter Δ:

(1) For $0 < \Delta < 1$, the interaction forces between different particle types are unequal in magnitude but remain opposite in direction, thereby preserving the character of the interaction-repulsive forces remain repulsive, and attractive forces remain attractive.

(2) For $\Delta > 1$, the nonreciprocity dominates, reversing the effective force direction. In this regime, a particle experiencing an attractive force exerts a repulsive one in return, resembling predator-prey-like interactions commonly observed in nature.

Furthermore, the net nonreciprocal force between particle pairs increases linearly with Δ.

In order to characterize the diffusion behavior of particles, we adopted the time-dependent MSD, defined as follows [3]:

$$\langle \Delta \mathbf{r}^2(t) \rangle = \frac{1}{N} \left\langle \sum_{i=1}^{N} |\mathbf{r}_i'(t) - \mathbf{r}_i'(0)|^2 \right\rangle, \tag{6}$$

where N is particle number. The calculations are performed in the center-of-mass reference frame, represented by $\mathbf{r}_{\text{cm}} = \frac{1}{N}\sum_i \mathbf{r}_i$, where $\mathbf{r}_i' = \mathbf{r}_i - \mathbf{r}_{\text{cm}}$. $\langle\cdot\rangle$ denote averaging over different initial conditions. This is to account for the global drift that arises due to momentum nonconservation in nonreciprocal systems; this drift will be analyzed in detail later. The effective diffusion coefficient, denoted as $D_{\text{eff}} = \lim_{t\to\infty} \frac{\langle \Delta \mathbf{r}^2(t) \rangle}{4t}$, is derived from long-time behavior. The transition from subdiffusive to normal diffusive behavior in MSD is a typical characteristic of glassy systems. When particles sense the presence of other particles, their motion becomes constrained, causing them to vibrate within the cage formed by neighboring particles. During this intermediate period, the MSD becomes flat and shows subdiffusive behavior before eventually transitioning to diffusive motion over a long timescale.

Another common feature of glassy systems is their long relaxation times, which can be characterized using the self-intermediate scattering function [29]:

$$F_s(k,t) = \frac{1}{N} \left\langle \sum_{i=1}^{N} e^{i\mathbf{k}\cdot(\mathbf{r}_i'(t) - \mathbf{r}_i'(0))} \right\rangle, \tag{7}$$

where the wave number k corresponds to the main peak of the structure factor. The relaxation time τ_α is determined by $F_s(k, \tau_\alpha) = e^{-1}$.

Dynamical heterogeneity is also a notable characteristic of glass systems. We utilize the non-Gaussian parameter to examine the heterogeneity of supercooled liquid dynamics, which is defined in two dimensions as [48]

$$\alpha_2(t) = \frac{\langle \Delta \mathbf{r}^4(t) \rangle}{2\langle \Delta \mathbf{r}^2(t) \rangle^2} - 1. \tag{8}$$

For a simple liquid obeying a Gaussian distribution, $\alpha_2 = 0$. However, for a supercooled liquid, $\alpha_2 > 0$, exhibiting interesting time and temperature dependencies.

In the simulation, we employ the stochastic Euler algorithm for the numerical integration of Eq. (1) with a time step of 10^{-4} and a total integration time of 4×10^5 to ensure the system reaches a nonequilibrium steady state. Particle positions are initialized by uniformly and randomly distributing them within the box, where $\rho = N/L^2$ denotes the particle number density in the box. Prior to data collection, we ensure that the system undergoes an equilibration period exceeding the structural relaxation time to reach a stable state. Unless otherwise stated, our simulations will use the following parameter settings: $\mu = 1$, $k_B = 1$, and $N = 1000$.

III. RESULTS AND DISCUSSION

The nonreciprocal interactions between particles greatly influence the system's dynamic behavior. Here, we primarily investigate (1) the impact of nonreciprocity on particle diffusion behavior under various density conditions and (2) the

effect of nonreciprocity on the glass dynamics of the system under dense conditions ($\rho = 1.2$).

A. Diffusion behavior

In Ref. [43], it was observed that at low densities, the self-diffusion coefficient increases with increasing nonreciprocity, and can exceed the theoretical upper limit, specifically the ideal diffusion coefficient predicted by the Stokes-Einstein theory. Additionally, Ref. [45] reported that at lower densities, nonreciprocity enhances the diffusion of tracer particles in nonreciprocal mixtures, with the diffusion coefficient monotonically increasing as the degree of nonreciprocity rises. This indicates that nonreciprocity significantly affects diffusion behavior under low-density conditions. It should be emphasized that this deviation primarily occurs in the dilute limit and reflects single-particle dynamics, which is distinct from the mechanism observed in dense glassy systems. In high-density glassy states, the breakdown of the Stokes-Einstein relation mainly arises from dynamic heterogeneity [49]. This heterogeneity leads to a decoupling between diffusion and structural relaxation, breaking the simple inverse relation predicted by the Stokes-Einstein theory.

In this study, we investigate how nonreciprocity affects self-diffusion under varying density conditions. We first consider the case of very low temperature (e.g., $T = 0.2$), and the results are depicted in Fig. 2(a). Generally, nonreciprocity facilitates particle diffusion as nonreciprocal forces, similar to active forces, that disrupt the system's equilibrium, leading to changes in particle positions and velocities, thereby promoting particle diffusion. In low-density conditions, the effective diffusion coefficient increases monotonically with an increase in nonreciprocity. Furthermore, when $\Delta > 1$, the diffusion coefficient tends to saturate. Interestingly, at high packing densities (e.g., $\rho = 1.1,\ 1.2$), the relationship between the effective diffusion coefficient and nonreciprocity becomes complex, exhibiting weak nonmonotonicity. As Δ increases from zero, the effective diffusion coefficient initially increases, then decreases, rises again, and ultimately reaches a saturation value. Notably, a decrease in the effective diffusion coefficient occurs around $\Delta = 0.2$ for $\rho = 1.1$ and $\Delta = 0.78$ for $\rho = 1.2$. This drop in the diffusion curve arises because, at high densities, the appropriate nonreciprocal interactions lead to the collective directed motion of the particles, thus diminishing their self-diffusion. It should be noted that as the density increases further (e.g., $\rho > 1.2$), particle repulsion becomes dominant, making the nonreciprocal coefficient ineffective when it is less than 1.0. As a result, this nonmonotonic behavior becomes less pronounced. A detailed discussion is provided in the analysis of Fig. 2(b).

To quantify the overall directional motion of particles, we define the drift velocity as $V_d = \lim_{t\to\infty} \frac{|\langle r_i(t)\rangle|}{t}$. The dependence of drift velocity V_d on Δ is illustrated in Fig. 2(b) for $T = 0.2$. The drift velocity exhibits a peak as a function of Δ. This can be ascribed to nonreciprocal interactions, which lead to directional particle motion at high densities, while concurrently generating nonequilibrium random forces that oppose this motion [44]. As Δ increases from zero, V_d gradually increases with Δ, primarily due to the directional motion induced by nonreciprocity. However, when Δ continues to increase beyond a certain point, V_d begins to decrease. This is because nonreciprocity generates the additional random force [44], and as this random force gradually strengthens and eventually becomes significant, it counteracts the directional motion. Therefore, there exists a specific value of Δ at which V_d reaches its maximum. From Eq. (6), it is evident that when calculating the MSD, the directional motion is subtracted, thereby the peak of the drift velocity indicates a decline in the diffusion coefficient, as shown in Fig. 2(a).

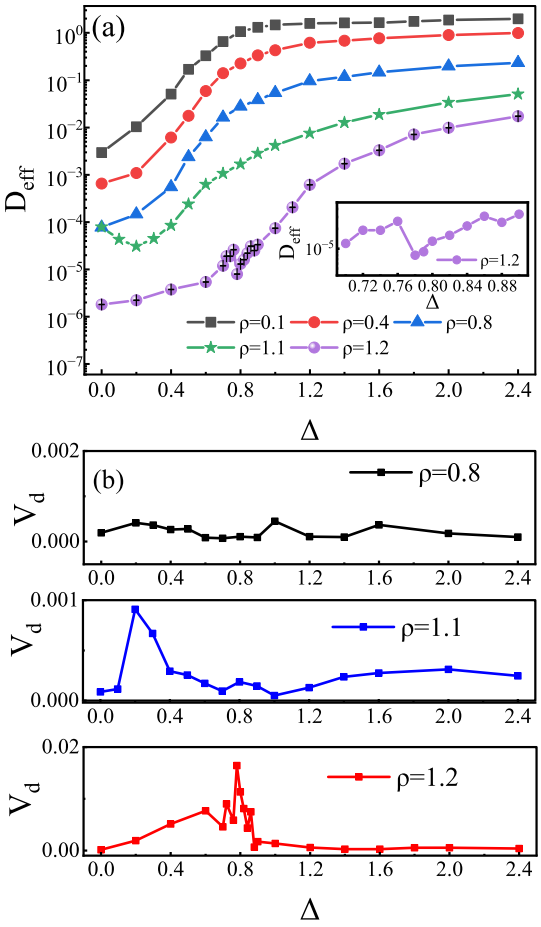

FIG. 2. (a) The effective diffusion coefficient D_{eff} as a function of the degree of nonreciprocity Δ for different ρ at $T = 0.2$. The inset shows a detailed close-up of the $\rho = 1.2$ curve. (b) The drift velocity V_d as a function of Δ for different ρ at $T = 0.2$.

To explain the drift motion caused by nonreciprocity, we have provided the distribution of the actual positions of the particles in Fig. 3 for different Δ at $\rho = 1.2$ and $T = 0.2$. In the absence of nonreciprocity ($\Delta = 0$), the particle distribution is almost symmetric. Due to the attraction between particles, they form a large cluster at low temperatures, with the center of this cluster located near the position (0,0). Therefore, the particle system exhibits no drift motion. When $\Delta = 0.8$, the nonreciprocal interactions generate nonequilibrium driving forces that are not sufficient to overcome the attraction between particles. As a result, the particles still form a cluster. However, this nonequilibrium driving leads to the appearance of traveling states, causing drift motion. As shown in the middle panel of Fig. 3, the center of the entire

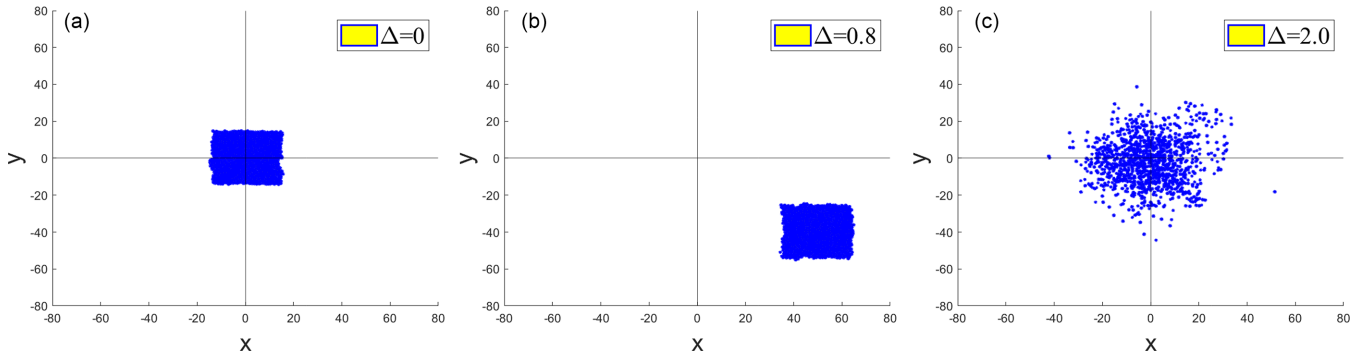

FIG. 3. Particle position distribution at $t = 5000.0$ for different Δ at $\rho = 1.2$ and $T = 0.2$: (a) $\Delta = 0$, (b) $\Delta = 0.8$, and (c) $\Delta = 2.0$. Note that here the particle positions refer to the actual positions of the particles, not their positions after applying the minimum image convention. Note: Particle coordinates have been unwrapped and centered, so the distribution may visually exceed the periodic box (28.8×28.8) boundaries. All particles remain confined within the box during simulation.

cluster has shifted away from its original position at (0,0). However, when the nonreciprocity is sufficiently strong (e.g., $\Delta = 2.0$), the nonequilibrium drive caused by nonreciprocity can overcome the attraction between particles, thereby disrupting the cluster. In this case, the nonreciprocal interactions do not produce traveling states. Although the particle motion speeds up, the central position of the entire particle system remains near $(0, 0)$, and no drift motion occurs. Therefore, the system will produce drift motion only when nonreciprocal interactions and particle-forming clusters are simultaneously satisfied.

To further validate the structural evolution underlying the observed drift behavior, we analyze the radial distribution function $g(r)$ at $T = 0.2$ for various values of Δ, as shown in Fig. 4. The height of the first peak of $g(r)$ exhibits a nonmonotonic dependence on Δ: it initially increases, reaches a maximum at intermediate Δ, and subsequently decreases. This observation suggests that moderate nonreciprocal interactions enhance local structural order, resulting in more compact particle arrangements. This is consistent with the cluster formation and directional drift behavior observed in Fig. 3. However, as Δ further increases, the strong nonequilibrium driving forces become strong enough to overcome the attractive interactions between particles, disrupting the cluster structure and consequently reducing the height of the first peak in $g(r)$.

Note that in Figs. 2(a) and 2(b), we consider a very low temperature scenario. However, under high-temperature conditions [e.g., $T = 0.5$, 0.7, 1.0 in Fig. 5(a)], even in dense regimes, the effective diffusion coefficient monotonically increases with Δ and does not exhibit any reduction in the

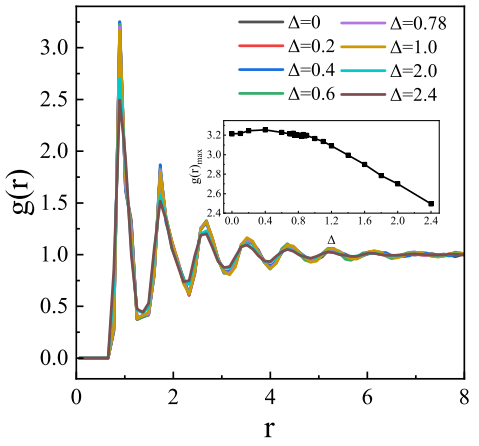

FIG. 4. The variation of radial distribution functions $g(r)$ with distance r for different nonreciprocity parameters Δ at $\rho = 1.2$ and $T = 0.2$. The inset shows the dependence of the first peak of $g(r)$ on Δ.

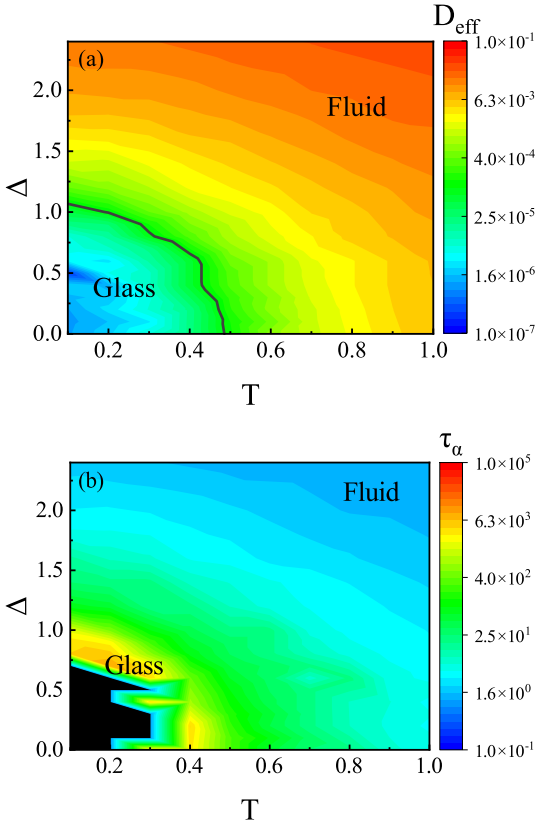

FIG. 5. (a) Heat map of the effective diffusion coefficient D_{eff} in the T–Δ representation. The black solid line represents the contour line of $D_{\text{eff}} = 10^{-4}$. (b) Heat map of the relaxation time τ_α in the T–Δ representation. The black area represents a high τ_α value.

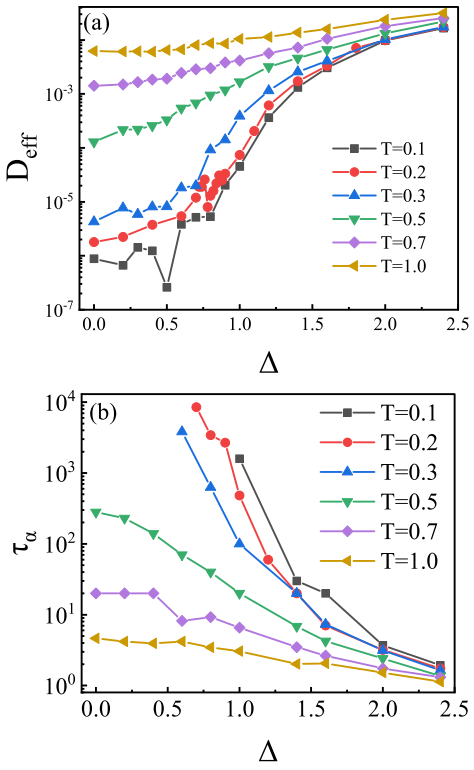

FIG. 6. (a) The effective diffusion coefficient D_{eff} as a function of Δ for different T. (b) The relaxation time τ_α as a function of Δ for different T. The other parameter is $\rho = 1.2$.

trajectory. A comprehensive analysis allows us to distill the following patterns: if the system is in a supercooled liquid state (signified by extremely low temperature and high density), the relationship between the effective diffusion coefficient and nonreciprocity is not monotonic, manifesting a dip in the middle of the D_{eff}–Δ graph. Conversely, in a hot liquid state (high temperature and density) or a gaseous state (low density), the effective diffusion coefficient uniformly rises with increasing Δ.

B. Glass dynamics

We next investigate the effect of nonreciprocity on the glass dynamics of the system under dense conditions ($\rho = 1.2$). As shown in Fig. 5, we present a comprehensive heat map to clearly illustrate the results. The heat maps of D_{eff} and τ_α in the T–Δ representation are shown in Figs. 5(a) and 5(b), respectively. In a glassy state, the system exhibits very small diffusion ($D_{\text{eff}} < 10^{-4}$) and long relaxation times, while in a liquid state, the system shows larger diffusion coefficients and shorter relaxation times. However, it should be emphasized that the standard definition of a glass state requires the absence of any measurable relaxation within experimentally feasible timescales. Since relaxation processes remain observable in our simulations, a more accurate description of this regime is a "viscous liquid." Accordingly, we designate the parameter region with $D_{\text{eff}} < 10^{-4}$ as the viscous liquid region, characterized by a long relaxation time for $F_s(k, t)$ and an extended plateau in the MSD over time. From Figs. 5(a) and 5(b), we can determine under which conditions the system is in the viscous liquid and under which conditions it is in the liquid state. The system appears to be in a viscous liquid when $T < 0.5$ and $\Delta < 1$. At high temperatures and high nonreciprocity, the system resides in a liquid state. Only at low temperatures (e.g., $T < 0.5$) can the system transition between the viscous liquid state and the liquid state by adjusting nonreciprocity.

To further detail and substantiate our findings, we provide the curves of D_{eff} and Δ at different temperatures in Fig. 6(a). As shown in Figs. 6(a) and 6(b), in high-temperature conditions (e.g., $T = 0.5$, 0.7, and 1.0), regardless of any changes to Δ, the system always remains in a liquid state. In low-temperature conditions (e.g., $T = 0.1$, 0.2, and 0.3), as Δ increases from zero, the system undergoes a transition from the viscous liquid to the liquid state. In other words, at low temperatures, nonreciprocal interactions can lead to a transition between the glassy state and the liquid state.

A similar dynamical acceleration induced by increasing Δ has also been observed in reciprocal active systems. For instance, in models such as active Brownian particles (ABPs) and active Ornstein-Uhlenbeck particles (AOUPs), increasing the activity strength or persistence time typically leads to

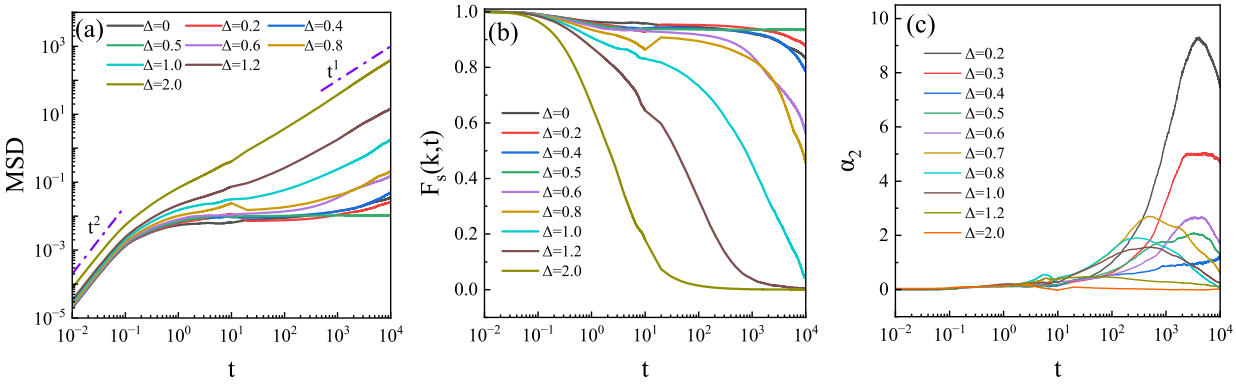

FIG. 7. Dynamics for different Δ at $T = 0.1$. (a) MSD as a function of time t for different Δ. (b) The self-intermediate scattering function of the majority A species as a function of t for different Δ. (c) The non-Gaussian parameter as a function of time t for different Δ. The height of the peak in $\alpha_2(t)$ is an indicator for dynamical heterogeneity, while a value of zero corresponds to diffusive motion. The other parameter is $\rho = 1.2$.

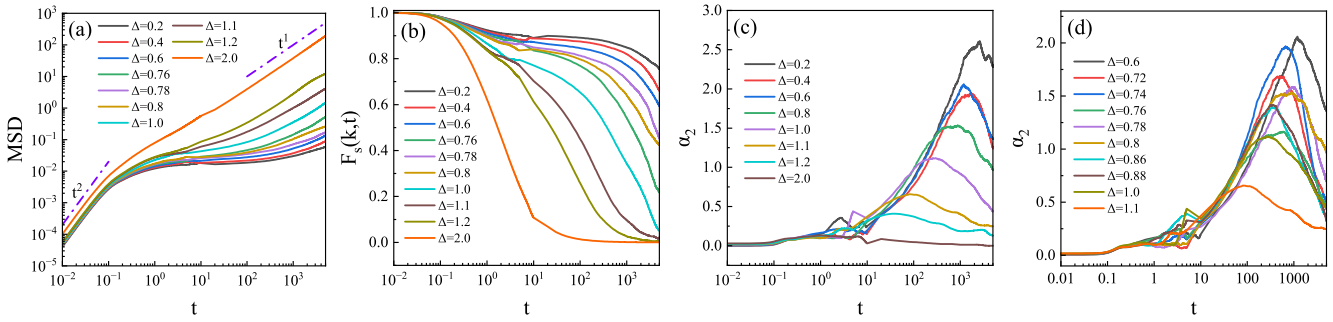

FIG. 8. Dynamics for different Δ at $T = 0.2$. (a) MSD as a function of time t for different Δ. (b) The self-intermediate scattering function of the majority A species as a function of t for different Δ. (c), (d) The non-Gaussian parameter as a function of time t for different Δ. The other parameter is $\rho = 1.2$.

enhanced diffusion, faster relaxation, and a tendency toward fluidization of the glassy state [16–21]. However, under high-density conditions, we find that the influence of nonreciprocal interactions on diffusion exhibits a nonmonotonic behavior: When Δ lies in an intermediate range, the system exhibits notably suppressed diffusion. Such behavior is uncommon in reciprocal active systems like ABPs and AOUPs. This suppression arises from the violation of action-reaction symmetry by nonreciprocal interactions, which promote the formation of collectively drifting clusters that hinder random diffusion. Therefore, although increasing Δ appears to induce a fluidization trend similar to that caused by an increase in effective temperature, the nonreciprocal system exhibits distinct complexities and differences.

To accurately describe the state of the system, we focus on the relationship between MSD, the intermediate scattering function, and the non-Gaussian parameter over time. Figures 7 and 9 display the system's dynamics at $T = 0.1$ and $T = 0.5$, respectively. As seen in Fig. 7 for $T = 0.1$, at $\Delta = 0$, 0.2, 0.4, and 0.6, $F_s(k, t)$ exhibits long relaxation times, the MSD shows a plateau, and high non-Gaussian parameters α_2 indicate strong dynamic heterogeneity. This suggests that the system is in a dynamically arrested viscous liquid. Contrarily, for $\Delta = 1.2$ and 2.0, short relaxation times for $F_s(k, t)$, linear time dependence of the MSD, and reduced non-Gaussian parameters suggest a diffusive system akin to a fluid. Thus, by modulating Δ, one can facilitate the system's transition between viscous liquid and liquid states. However, as depicted in Fig. 9 for $T = 0.5$, changes in Δ do not impact the system's short relaxation times for $F_s(k, t)$, MSD increases linearly with time, and there are negligible non-Gaussian parameters, which are indicative of fluidity. The acceleration of particle motion caused by a rise in T enhances diffusion and prompts the transition from the viscous liquid ($T = 0.1$) to the liquid state ($T = 0.5$).

To gain deeper insight into the dynamical features corresponding to the minimum of the effective diffusion coefficient D_{eff}, we further analyzed the MSD, self-intermediate scattering function $F_s(k, t)$, and non-Gaussian parameter α_2 within this regime. As shown in Fig. 7, at $T = 0.1$ and $\Delta = 0.5$, the MSD exhibits ballistic growth at short times followed by a pronounced plateau at longer times, indicating a significant suppression of particle diffusion [Fig. 7(a)]. Correspondingly, $F_s(k, t)$ decays slowly, reflecting markedly delayed structural relaxation [Fig. 7(b)]. Although the non-Gaussian parameter's peak values show an overall decreasing trend, they display irregular fluctuations near $\Delta = 0.5$ [Fig. 7(c)]. Complementary analysis at $T = 0.2$ reveals that at $\Delta = 0.78$, the MSD plateau persists longer than at neighboring Δ values [Fig. 8(a)], and $F_s(k, t)$ similarly exhibits

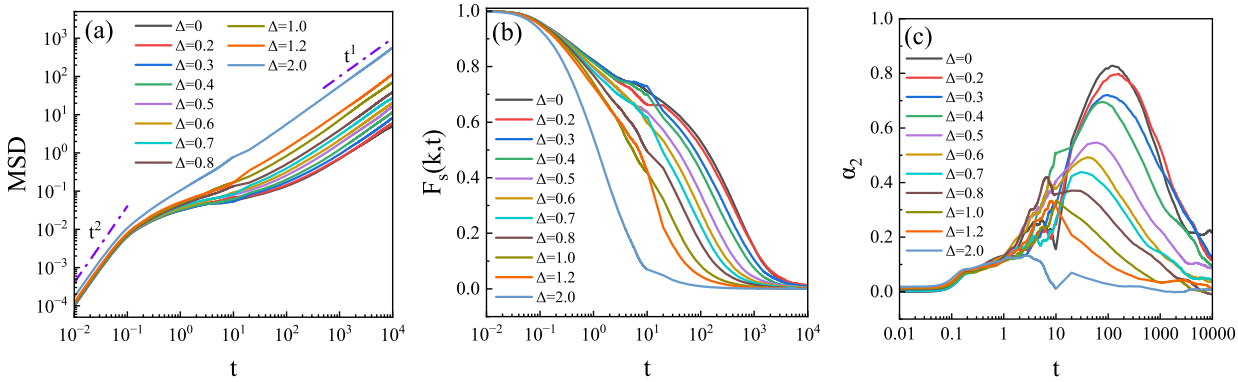

FIG. 9. Dynamics for different Δ at $T = 0.5$. (a) MSD as a function of time t for different Δ. (b) The self-intermediate scattering function of the majority A species as a function of t for different Δ. (c) The non-Gaussian parameter as a function of time t for different Δ. The other parameter is $\rho = 1.2$.

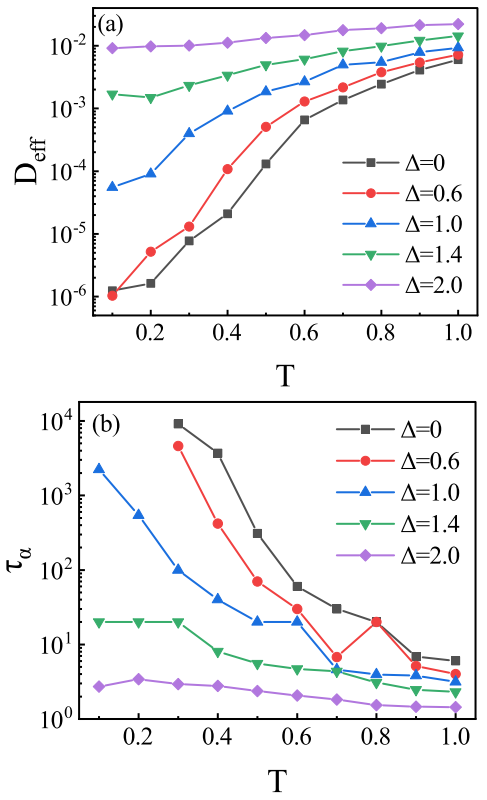

FIG. 10. (a) The effective diffusion coefficient D_{eff} as a function of T for different Δ. (b) The relaxation time τ_α as a function of T for different Δ. The other parameter is $\rho = 1.2$.

slow decay [Fig. 8(b)]. Likewise, the non-Gaussian parameter's peak values also decrease gradually overall [Fig. 8(c)], but exhibit irregular fluctuations near $\Delta = 0.78$ [Fig. 8(d)], indicating an impact on dynamical heterogeneity. Notably, at the higher temperature $T = 0.5$ (Fig. 9), the peak values of the non-Gaussian parameter do not exhibit such fluctuations, further confirming that these dynamical anomalies are only in the low-temperature regime. This distinct dynamical state originates from the competition between two types of driving forces induced by nonreciprocal interactions: one is a directed drift promoting coherent collective motion of particles, and the other is a stochastic nonequilibrium random force. The interplay between these forces governs particle diffusion and dynamical heterogeneity—while the ordered driving force suppresses random diffusion, the stochastic force increases system disorder, leading to irregular fluctuations in the peak values of the non-Gaussian parameter.

Similarly, we will present detailed diagrams illustrating the effect of temperature T on the glass transition across various Δ values. Figure 10(a) demonstrates that at low temperatures, nonreciprocity significantly influences particle diffusion behavior. Increasing Δ from 0 to 2 raises the diffusion coefficient from 10^{-6} to 10^{-2}. As a result, adjusting Δ can induce the system to transition from a viscous liquid state to a liquid state. Conversely, at higher temperatures, the effect of nonreciprocity on particle diffusion is minimal. This observation is corroborated by the relaxation time τ_α depicted in Fig. 10(b), where at low temperatures, changes in Δ lead to multiple orders of magnitude variations in τ_α. However, at higher temperatures, the relaxation time changes due to Δ variations are modest, and the relaxation times remain consistently low.

Figure 11 presents the MSD, intermediate scattering function, and non-Gaussian parameter as functions of time t at $\Delta = 0$. It is observed that as the temperature increases from 0.1, the MSD plateau diminishes and eventually disappears, the relaxation time plateau decreases, and the peak of the non-Gaussian parameter reduces. These changes indicate the system's transformation from a viscous liquid state to a liquid state. As the temperature continues to rise, the system evolves from a highly viscous liquid state to a hot liquid state.

IV. CONCLUDING REMARKS

In conclusion, our investigation focused on studying diffusion and glass transition phenomena within a two-dimensional Kob-Andersen mixture featuring nonreciprocal particle interactions. We have discovered that nonreciprocal interactions significantly influence particle dynamics. (1) Concerning diffusion, our findings reveal intriguing behaviors: In the supercooled liquid state, characterized by extremely low temperature and high density, the relationship between the effective diffusion coefficient and nonreciprocity is weakly nonmonotonic, exhibiting a decrease in the middle of the D_{eff}–Δ curve. Conversely, in the hot liquid state or in the gaseous state, the effective diffusion coefficient monotonically increases with the increasing Δ. (2) Regarding glass

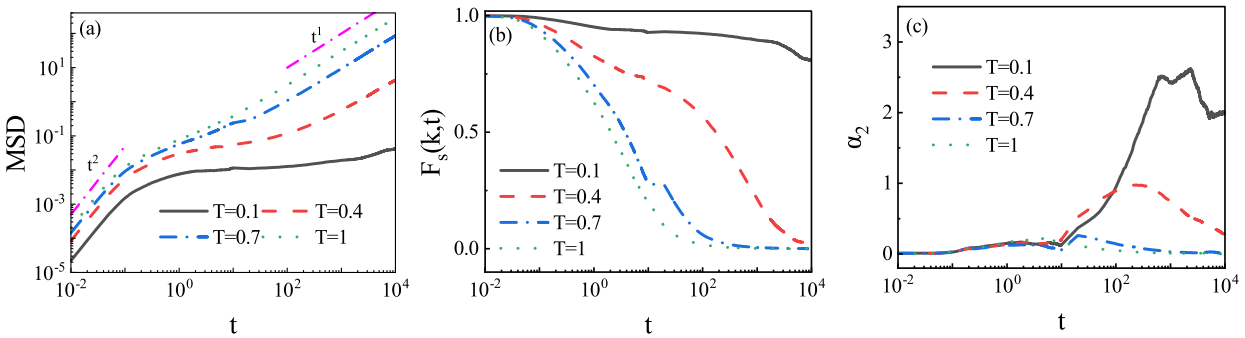

FIG. 11. Dynamics for different T at $\Delta = 0$. (a) MSD as a function of time t for different T. (b) The self-intermediate scattering function of the majority A species as a function of t for different T. (c) The non-Gaussian parameter as a function of time t for different T. The other parameter is $\rho = 1.2$.

dynamics, our observations demonstrate two distinct states: The system exhibits a viscous liquid state when $T < 0.5$ and $\Delta < 1$, while at high temperatures and high nonreciprocity, it transitions into a liquid state. Notably, the transition between the glass and liquid states by altering nonreciprocity occurs only at low temperatures (e.g., $T < 0.5$).

These findings underscore the intricate interplay between particles and system dynamics, shedding light on the nuanced behaviors observed in supercooled liquids undergoing glass transition. Our results provide valuable insights into the role of nonreciprocal interactions in governing diffusion and glass transition phenomena, thereby contributing to a deeper understanding of complex systems in statistical physics. Further investigations into the mechanisms underlying these phenomena could yield important implications across various fields, ranging from materials science to biophysics. At present, this remains a theoretical concept, and experimental validation in nonreciprocal systems should be pursued [36,39].

ACKNOWLEDGMENTS

This work was supported in part by the National Natural Science Foundation of China (Grants No. 12075090, No. 12475036, No. 12275064, and No. 12265017) and the Guangdong Basic and Applied Basic Research Foundation (Grants No. 2022A1515010449 and No. 2024A1515012575).

DATA AVAILABILITY

The data that support the findings of this article are openly available [50]; embargo periods may apply.

[1] L. Berthier and G. Biroli, Theoretical perspective on the glass transition and amorphous materials, Rev. Mod. Phys. **83**, 587 (2011).
[2] A. Burin, Glassy materials and disordered solids: An introduction to their statistical mechanics, Phys. Today **59**(9), 64 (2006).
[3] E. Flenner and G. Szamel, Relaxation in a glassy binary mixture: Comparison of the mode-coupling theory to a Brownian dynamics simulation, Phys. Rev. E **72**, 031508 (2005).
[4] F. Sciortino, W. Kob, and P. Tartaglia, Inherent structure entropy of supercooled liquids, Phys. Rev. Lett. **83**, 3214 (1999).
[5] L. Berthier, Time and length scales in supercooled liquids, Phys. Rev. E **69**, 020201 (2004).
[6] R. K. Murarka and B. Bagchi, Pair dynamics in a glass-forming binary mixture: Simulations and theory, Phys. Rev. E **67**, 041501 (2003).
[7] E. Flenner and G. Szamel, Fundamental differences between glassy dynamics in two and three dimensions, Nat. Commun. **6**, 7392 (2015).
[8] L. Berthier and R. L. Jack, Structure and dynamics of glass formers: Predictability at large length scales, Phys. Rev. E **76**, 041509 (2007).
[9] S. Franz, R. Mulet, and G. Parisi, Kob-Andersen model: A nonstandard mechanism for the glassy transition, Phys. Rev. E **65**, 021506 (2002).
[10] L. M. C. Janssen, Active glasses, J. Phys.: Condens. Matter **31**, 503002 (2019).
[11] N. Klongvessa, F. Ginot, C. Ybert, C. Cottin-Bizonne, and M. Leocmach, Active glass: Ergodicity breaking dramatically affects response to self-propulsion, Phys. Rev. Lett. **123**, 248004 (2019).
[12] B. R. Parry, I. V. Surovtsev, M. T. Cabeen, C. S. O'Hern, E. R. Dufresne, and C. Jacobs-Wagner, The bacterial cytoplasm has glass-like properties and is fluidized by metabolic activity, Cell **156**, 183 (2014).
[13] T. E. Angelini, E. Hannezo, X. Trepat, M. Marquez, J. J. Fredberg, and D. A. Weitz, Glass-like dynamics of collective cell migration, Proc. Natl. Acad. Sci. USA **108**, 4714 (2011).
[14] S. Grosser, J. Lippoldt, L. Oswald, M. Merkel, D. M. Sussman, F. Renner, P. Gottheil, E. W. Morawetz, T. Fuhs, X. Xie, S. Pawlizak, A. W. Fritsch, B. Wolf, L.-C. Horn, S. Briest, B. Aktas, M. L. Manning, and J. A. Käs, Cell and nucleus shape as an indicator of tissue fluidity in carcinoma, Phys. Rev. X **11**, 011033 (2021).
[15] L. Berthier and J. Kurchan, Non-equilibrium glass transitions in driven and active matter, Nat. Phys. **9**, 310 (2013).
[16] R. Ni, M. A. Cohen Stuart, and M. Dijkstra, Pushing the glass transition towards random close packing using self-propelled hard spheres, Nat. Commun. **4**, 2704 (2013).
[17] L. Berthier, Nonequilibrium glassy dynamics of self-propelled hard disks, Phys. Rev. Lett. **112**, 220602 (2014).
[18] E. Flenner, G. Szamel, and L. Berthier, The nonequilibrium glassy dynamics of self-propelled particles, Soft Matter **12**, 7136 (2016).
[19] L. Berthier, E. Flenner, and G. Szamel, How active forces influence nonequilibrium glass transitions, New J. Phys. **19**, 125006 (2017).
[20] L. Berthier, E. Flenner, and G. Szamel, Glassy dynamics in dense systems of active particles, J. Chem. Phys. **150**, 200901 (2019).
[21] R. Mandal, P. J. Bhuyan, M. Rao, and C. Dasgupta, Active fluidization in dense glassy systems, Soft Matter **12**, 6268 (2016).
[22] G. Szamel, E. Flenner, and L. Berthier, Glassy dynamics of athermal self-propelled particles: Computer simulations and a nonequilibrium microscopic theory, Phys. Rev. E **91**, 062304 (2015).
[23] D. Bi, X. Yang, M. C. Marchetti, and M. L. Manning, Motility-driven glass and jamming transitions in biological tissues, Phys. Rev. X **6**, 021011 (2016).
[24] G. Szamel, Theory for the dynamics of dense systems of athermal self-propelled particles, Phys. Rev. E **93**, 012603 (2016).
[25] S. K. Nandi, R. Mandal, P. J. Bhuyan, C. Dasgupta, M. Rao, and N. S. Gov, A random first-order transition theory for an active glass, Proc. Natl. Acad. Sci. USA **115**, 7688 (2018).
[26] R. Mandal and P. Sollich, Multiple types of aging in active glasses, Phys. Rev. Lett. **125**, 218001 (2020).
[27] V. E. Debets, X. M. de Wit, and L. M. C. Janssen, Cage length controls the nonmonotonic dynamics of active glassy matter, Phys. Rev. Lett. **127**, 278002 (2021).
[28] V. E. Debets and L. M. C. Janssen, Active glassy dynamics is unaffected by the microscopic details of self-propulsion, J. Chem. Phys. **157**, 224902 (2022).

[29] V. E. Debets and L. M. C. Janssen, Influence of particle softness on active glassy dynamics, Phys. Rev. Res. **4**, L042033 (2022).

[30] G. Janzen and L. M. C. Janssen, Rejuvenation and memory effects in active glasses induced by thermal and active cycling, Phys. Rev. Res. **6**, 023257 (2024).

[31] V. E. Debets, H. Löwen, and L. M. C. Janssen, Glassy dynamics in chiral fluids, Phys. Rev. Lett. **130**, 058201 (2023).

[32] B. Q. Ai, R. X. Guo, C. H. Zeng, and Y. F. He, Rotational inertia-induced glassy transition in chiral particle systems, Phys. Rev. E **109**, 064902 (2024).

[33] R. X. Guo, J. J. Li, and B. Q. Ai, Diffusion of active particles driven by odd interactions, Phys. Rev. E **111**, 014105 (2025).

[34] R. A. Long and F. Azam, Antagonistic interactions among marine pelagic bacteria, Appl. Environ. Microbiol. **67**, 4975 (2001).

[35] A. Strandburg-Peshkin, C. R. Twomey, N. W. F. Bode, A. B. Kao, Y. Katz, C. C. Ioannou, S. B. Rosenthal, C. J. Torney, H. S. Wu, S. A. Levin, and I. D. Couzin, Visual sensory networks and effective information transfer in animal groups, Curr. Biol. **23**, R709 (2013).

[36] G. Gardi and M. Sitti, On-demand breaking of action-reaction reciprocity between magnetic microdisks using global stimuli, Phys. Rev. Lett. **131**, 058301 (2023).

[37] A. V. Ivlev, J. Bartnick, M. Heinen, C. R. Du, V. Nosenko, and H. Löwen, Statistical mechanics where Newton's third law is broken, Phys. Rev. X **5**, 011035 (2015).

[38] Z. You, A. Baskaran, and M. C. Marchetti, Nonreciprocity as a generic route to traveling states, Proc. Natl. Acad. Sci. USA **117**, 19767 (2020).

[39] C. H. Meredith, P. G. Moerman, J. Groenewold, Y. J. Chiu, W. K. Kegel, A. van Blaaderen, and L. D. Zarzar, Predator–prey interactions between droplets driven by non-reciprocal oil exchange, Nat. Chem. **12**, 1136 (2020).

[40] R. Mandal, S. S. Jaramillo, and P. Sollich, Robustness of traveling states in generic nonreciprocal mixtures, Phys. Rev. E **109**, L062602 (2024).

[41] R. K. Gupta, R. Kant, H. Soni, A. K. Sood, and S. Ramaswamy, Active nonreciprocal attraction between motile particles in an elastic medium, Phys. Rev. E **105**, 064602 (2022).

[42] K. L. Kreienkamp and S. H. L. Klapp, Clustering and flocking of repulsive chiral active particles with non-reciprocal couplings, New J. Phys. **24**, 123009 (2022).

[43] Y. J. Chiu and A. K. Omar, Phase coexistence implications of violating Newtons third law, J. Chem. Phys. **158**, 164903 (2023).

[44] B. Q. Ai, Brownian motors powered by nonreciprocal interactions, Phys. Rev. E **108**, 064409 (2023).

[45] A. Benois, M. Jardat, V. Dahirel, V. Démery, J. Agudo-Canalejo, R. Golestanian, and P. Illien, Enhanced diffusion of tracer particles in nonreciprocal mixtures, Phys. Rev. E **108**, 054606 (2023).

[46] L. Cocconi, H. Alston, and T. Bertrand, Active bound states arising from transiently nonreciprocal pair interactions, Phys. Rev. Res. **5**, 043032 (2023).

[47] J. Chen, X. Lei, Y. Xiang, M. Duan, X. Peng, and H. P. Zhang, Emergent chirality and hyperuniformity in an active mixture with nonreciprocal interactions, Phys. Rev. Lett. **132**, 118301 (2024).

[48] L. J. Wang, Y. H. Duan, and N. Xu, Non-monotonic pressure dependence of the dynamics of soft glass-formers at high compressions, Soft Matter **8**, 11831 (2012).

[49] P. Chaudhuri, L. Berthier, and W. Kob, Universal nature of particle displacements close to glass and jamming transitions, Phys. Rev. Lett. **99**, 060604 (2007).

[50] R.-X. Guo, J.-J. Li, C.-H. Zeng, Y.-F. He, and B.-Q. Ai, Nonmonotonic effects of nonreciprocal interactions on glass transition and diffusion in a two-dimensional emergent active system [Dataset], Zenodo (2025), https://doi.org/10.5281/zenodo.17128308.